

Supporting Information for “Emergent ionic conduction in aliovalently-doped fast ion  
conductors”

Bharathi Bandi and Abhijit Chatterjee\*

Department of Chemical Engineering, Indian Institute of Technology Bombay, Mumbai  
400076, Maharashtra

\*Email: [abhijit@che.iitb.ac.in](mailto:abhijit@che.iitb.ac.in)

S1. Construction of ionic layers

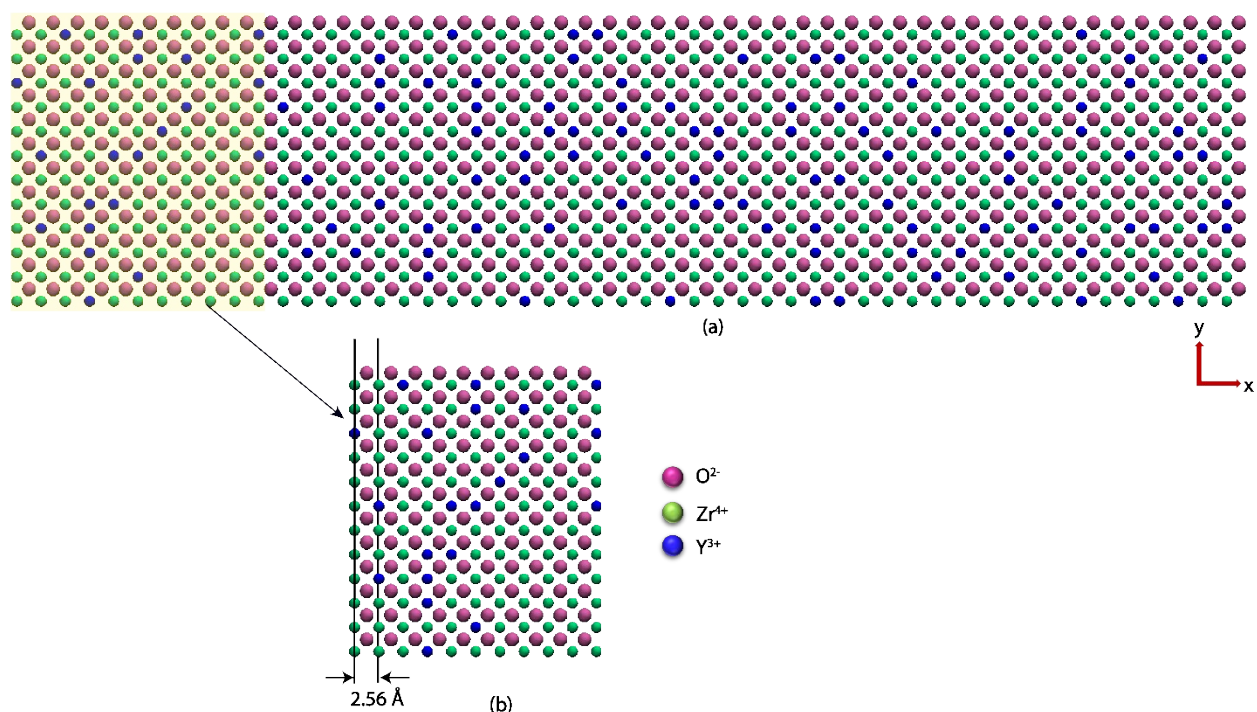


Figure S1. (a) YSZ bulk system ( $O^{2-}$  ions in dark pink,  $Zr^{4+}$  ions in green and  $Y^{3+}$  ions in blue, respectively), (b) Step1: Identifying ionic layers in the on-lattice YSZ bulk system.

Layer-wise division of the *on-lattice* bulk system has been performed as follows:

**Step 1:** Identify atomic layer in x-direction: Each layer position along x-axis is noted as shown in Figure S1b. In bulk YSZ, the alternate atomic layers contain anions ( $O^{2-}$ ) and cations ( $Zr^{4+}$  or  $Y^{3+}$ ). Cations are immobile. Oxide ions hop from one anion site to other. The bin/layer boundary is such that anion site is at the center of the bin. The position of the cation layer is shown in the Table 1.

<b>Table 1: Ionic layer position for bulk YSZ system (see Figure S1a).</b>		
<b>Layer</b>	<b>Position of cation layer (x)</b>	<b><math>\Delta x_{\text{layer}}</math></b>
1	x1=0	
2	x2= 2.5675	2.5675
3	x3= 5.135	2.5675
4	x4= 7.7025	2.5675
5	x5=7.7025	2.5675
6	x6=10.27	2.5675
.	.	.
.	.	.
.	.	.
.	.	2.5675
98	x98=249.0475	

**Step 2:** Construction of bins along x-direction: Next, we create bins so that each anion ionic layer is centered within a bin (Figure S1b). Furthermore, bin-width is kept equal to ion layer separation. For Table 1 the bin width is,  $\Delta x = 2.567 \text{ \AA}$ . Each bin contains  $x_{\text{max}}$  and  $x_{\text{min}}$  and these details are mentioned in Table 2:

<b>Table 2: Bin division for the YSZ Bulk system shown in Figure S3a.</b>		
$x_{\text{min}}$	<b>Position of center O<sup>2-</sup> layer (x)</b>	$x_{\text{max}}$
0.000	1.283	2.5675
2.5675	3.851	5.135
5.135	6.418	7.7025
7.7025	8.986	10.27
10.27	11.553	12.8375
.	.	.
.	.	.
.	.	.
246.48	247.76	249.047

## **S2. Bridge site effect at microscopic local environment scale**



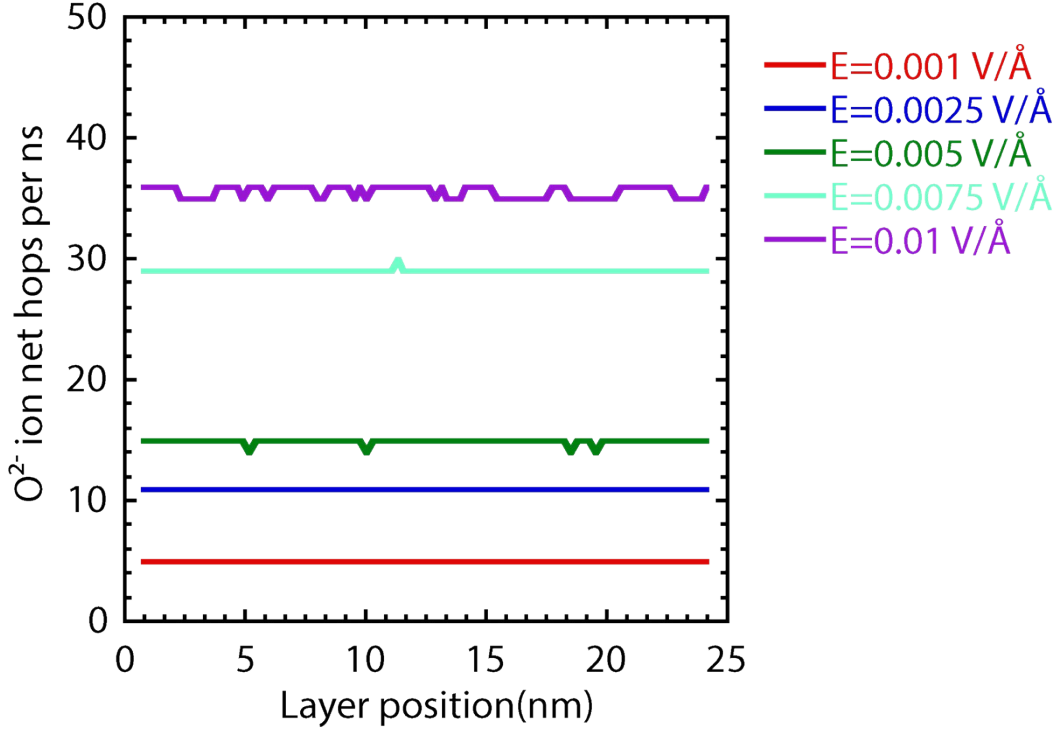


**Figure S3. Net hop events involving O<sup>2-</sup> ion in each layer of entire super cell**

Net hop events of O<sup>2-</sup> ions (which is related to  $\Delta F_o$ ) is shown in the Figure S3 for different applied electric fields.  $\Delta F_o$  increases with electric field. The value of  $\Delta F_o$  for any selected electric field is spatially uniform throughout the YSZ structure. This also indicates that the system has achieved steady state.

#### S4. Brønsted-Evans-Polanyi (BEP) relation

The BEP is a linear scaling relationship of the form

$$E_a = E_0 + \alpha \Delta H \quad (1)$$

where,

$E_0$  is the activation energy of reference configuration,  $\alpha$  characterizes the position of the transition state along the reaction coordinate (such that  $0 \leq \alpha \leq 1$ )

$\Delta H$  is the enthalpy change associated with a move in a configuration in question, and  $E_0$  is the corresponding activation energy.

When an oxygen ion hops from one anion site to its neighbor, the enthalpy associated with hopping of atoms is given by,

$$\Delta H = H_{final} - H_{initial}. \quad (2)$$

An external electric field is applied to the system,  $H_{final}$  can be written as:  $H_{final} = H_{final}^0 + q\lambda E_{ext}$ , where,

$q$  is charge of atom,

$\lambda$  is hopping distance, and

$E_{appl}$  is applied electric field.

$$\Delta H = H_{final}^0 + q\lambda E_{appl} - H_{initial}^0. \quad (3)$$

Finally,

$$\Delta H = \Delta H^0 + q\lambda E_{appl} \quad (4)$$

From the Eq. (1),

$$E_a = E_0 + \frac{1}{2}\Delta H. \quad (5)$$

Here, we have taken as  $\alpha = \frac{1}{2}$ .

$$E_a = E_0 + \frac{1}{2}(\Delta H^0 + q\lambda E_{appl}). \quad (6)$$

Writing  $E_a^0 = E_0 + \frac{1}{2}\Delta H^0$

$$E_a = E_a^0 + \frac{1}{2}q\lambda E_{appl}. \quad (7)$$

Using the Arrhenius relation, the kinetic rates associated with hopping events can be expressed as,

$$k = \nu e^{-\beta E_a}. \quad (8)$$

where,  $\beta = \frac{1}{k_B T}$ ,  $k_B$ =Boltzmann constant and  $T$ = temperature.

$$k(E_{appl}) = \nu e^{-\beta E_a^0} e^{-\frac{\beta q \lambda E_{appl}}{2}}. \quad (9)$$

Considering  $k(0) = \nu e^{-\beta E_a^0}$ ,

$$k(E_{appl}) = k(0) e^{-\frac{\beta q \lambda E_{appl}}{2}}. \quad (10)$$

$$\chi = e^{-\frac{\beta q \lambda E_{ext}}{2}}.$$

In the present study, the applied electric field is directed along the  $+x$  axis. A greater number of oxide ions are observed to move in the  $-x$  direction, resulting in a difference in the rates of movement along the  $+x$  and  $-x$  axes. The expressions for these rates are provided below,

$$k_{+x}(E_{appl}) = k_{+x}(0) e^{-\frac{\beta q \lambda E_{appl}}{2}}. \quad (11)$$

And

$$k_{-x}(E_{appl}) = k_{-x}(0) e^{-\frac{\beta q \lambda E_{appl}}{2}}. \quad (12)$$

$\chi$  is BEP factor for the oxygen ion hops at the microscopic length scales.

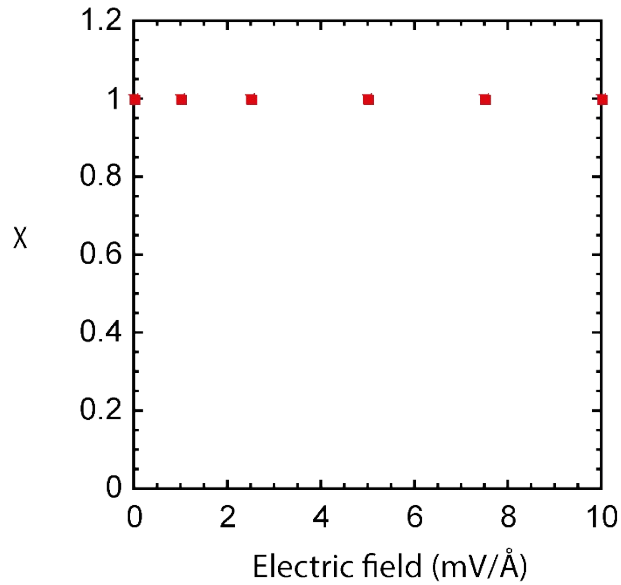


**Figure S4. BEP factor variation in presence of external electric field.**

Figure S4 shows the BEP factor for various applied electric field strength considered in the main text. There is not significant change in the BEP factor ( $\chi$ ) over applied electric field range. This is the reason why BEP is unable to show the microscopic behavior of hopping rates at local cation environments.

## S5. Oxide ion hopping in YSZ

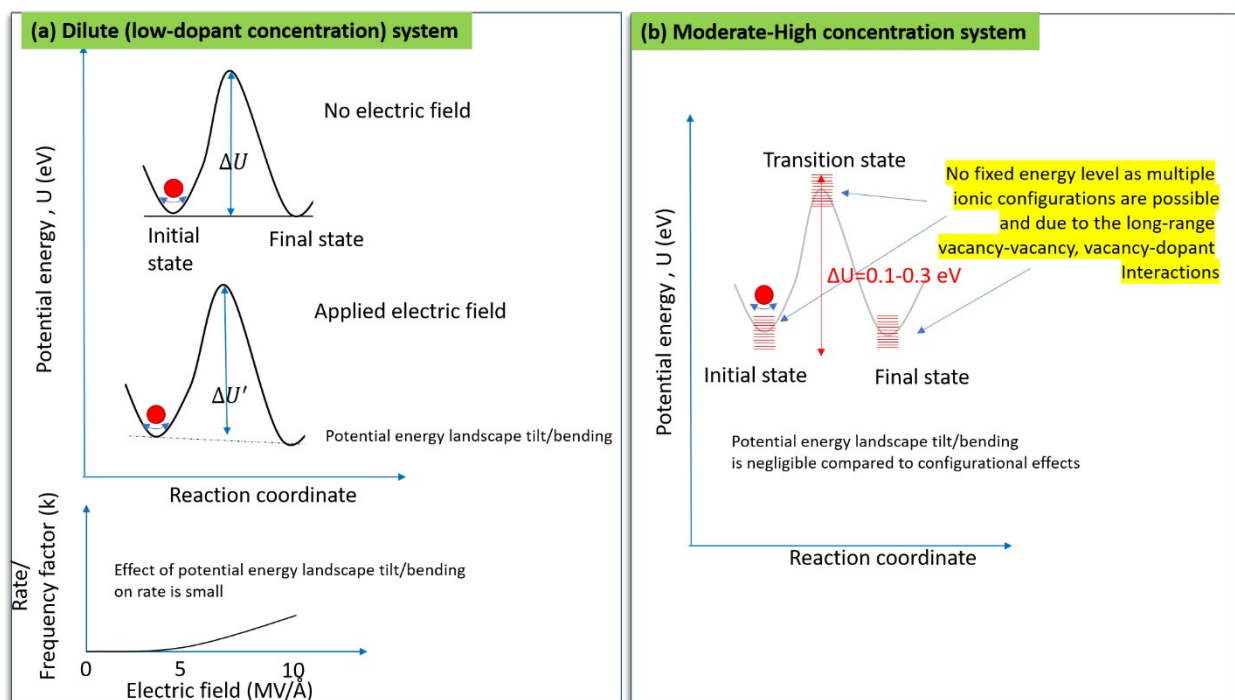


**Figure S5. Ion hopping potential landscapes for (a) dilute (low dopant) systems (b) moderately-high dopant concentration systems.**

A common picture used to describe the ion hopping process in a solid-state material with low vacancy defect concentration involves a potential energy landscape as shown in Figure S5a. Ion hopping is thermally-activated, i.e., an activation barrier needs to be overcome. The potential energy landscape is modified in presence of an external electric field. The effect of the external electric field is estimated using the Brønsted-Evans-Polanyi (BEP) relation. Such a simplistic picture cannot be extended to materials containing a high vacancy defect concentration as explained next.

First, it is important to recognize that the potential energy landscape in case of a hopping ion is dependent on the configuration of other ions in the vicinity. As a consequence, quantities such as formation energy, association energy and activation barrier will vary the local ionic configuration. The density functional theory study in Ref. <sup>3</sup> provides examples of the extent to

which vacancy-vacancy and vacancy-dopant interactions influence these energy quantities. From Ref. 3, one can conclude that the typical variation in energy can be around 0.1-0.3 eV, i.e., the rates are affected by a factor of 10 times at 1000 K. In contrast, the electric field can modify the hopping rate by a factor of 0.999-1.001 times (see Section S4 and bottom panel in Figure S5a).

Second, in YSZ an oxygen ion can hop at picosecond-nanosecond timescales, indicating that the local ionic configuration is highly dynamic. In view of this, a more appropriate potential energy diagram is shown in Figure S5b. The energy levels can vary with the local ionic configuration. This variation in  $\Delta U$  is expected to be between 0.1-0.3 eV, as mentioned above. Once again, the corresponding energy tilt/bending/shift will be  $\sim 0.0001$  eV. We have presented an analysis of the Brønsted-Evans-Polanyi (BEP) relation (see Supporting Information S4). This demonstrates that the changes in hopping frequency/rate constant due to the applied electric field is not as pronounced as that due to the configuration aspects.

In view of the above, given that a plethora of ionic configurations is possible, a free energy landscape is more appropriate to better understand the ion hopping process under the influence of an electric field. In this picture, the effect of background oxygen ions, vacancy defects and cations are captured in a statistically averaged manner. In our earlier studies<sup>4,5</sup>, we have linked free energy, hopping rate ( $k$ ), and O-V pair probabilities ( $\pi$ ) at zero electric fields. Upon applying an electric field, the key effect is that the configuration of the mobile ions changes and this affects the rate. Our analysis captures the effect of the configurational changes on the hopping frequency/rate constant.

### S6 Expression for anion pair probability from mean field theory (MFT)

8 mol %  $Y_2O_3$  doped  $ZrO_2$  in the form of equation:

$$Y_x Zr_{1-x} O_{2-\frac{x}{2}} \quad (13)$$

From the Eq. (13),

The probability of O in anion site is,

$$P_O = \frac{\text{Moles of O anion}}{\text{Total moles of anions}} \quad (14)$$

$$P_O = \frac{2 - x/2}{2} = \left(1 - \frac{x}{4}\right) \quad (15)$$

Similarly, the probability of vacancy in an anion site written as,



$$P_V = \frac{x/2}{2} = \frac{x}{4}. \quad (16)$$

The type of anion pairs possible in the YSZ system is  $O-O$ ,  $O-V$ ,  $V-O$ , and  $V-V$ . the sum of pair probabilities is equal to 1. Note here  $P_{O-V} = P_{V-O}$ .

$$P_{O-O} + 2P_{O-V} + P_{V-V} = 1 \quad (17)$$

$$P_{O-O} = \left(1 - \frac{x}{4}\right) * \left(1 - \frac{x}{4}\right) \quad (18)$$

$$P_{O-V} = \left(1 - \frac{x}{4}\right) * \left(\frac{x}{4}\right) \quad (19)$$

$$P_{V-V} = \left(\frac{x}{4}\right) * \left(\frac{x}{4}\right) \quad (20)$$

As  $x = 0.16$ , this follows:

$$P_{O-O} = 0.9216$$

$$P_{O-V} = 0.0384$$

$$P_{V-V} = 0.0016$$

$$\text{And } P_{O-O} + 2P_{O-V} + P_{V-V} = 0.9216 + (2 * 0.0384) + 0.0016 = 1$$

## S7. Standard model for ionic conductivity in dilute systems

A standard model for ionic conduction at low dopant concentrations is

$$\sigma = \frac{1}{6} \frac{f_d C q^2}{H_R k_B T} a^2 v_o \exp\left(\frac{\Delta S}{k_B}\right) \exp\left(\frac{-\Delta H}{k_B T}\right). \quad (2)$$

where,

$C$ = Concentration of charge carrier,

$q$ = charge,

$k_B$ = Boltzman constant,

$T$ =Temperature,

$a$ = lattice constant,

$\nu_o$ =frequency factor,

$\Delta S$ =entropy term,

$\Delta H$ =enthalpy term,

$f_d$ =Tracer corelation coefficient, and

$H_R$ =Haven ratio

In superficial and interfacial superionic conductors, structural differences at the interfaces lead to lattice volume expansion and the accumulation of ions, such as Li, at the interface, enhancing ionic conductivity. In the case of Li-ion interfacial superconductors, it has been shown that the increase in interfacial ionic conductivity enhances fast charging capabilities<sup>6</sup>.

## Reference

- 1 M. Jaipal and A. Chatterjee, *J. Phys. Chem. C*, 2017, **121**, 14534–14543.
- 2 M. Jaipal and A. Chatterjee, *Model. Simul. Mater. Sci. Eng.*, 2019, **27**, 64003.
- 3 A. Bogicevic and C. Wolverton, *Phys. Rev. B*, 2003, **67**, 024106.
- 4 M. Jaipal and A. Chatterjee, *J. Phys. Chem. C*, 2017, **121**, 14534–14543.
- 5 M. Jaipal, B. Bandi and A. Chatterjee, *Phys. Chem. Chem. Phys.*, 2021, **23**, 3716–3728.
- 6 H. Kwak, J. S. Kim, D. Han, J. S. Kim, J. Park, G. Kwon, S. M. Bak, U. Heo, C. Park, H. W. Lee, K. W. Nam, D. H. Seo and Y. S. Jung, *Nat. Commun.*, 2023, **14**, 1–14.